AJSM PreView, published on February 7, 2013 as doi:10.1177/0363546512473572

Isolation and Characterization of 2 New Human Rotator Cuff and Long Head of Biceps Tendon Cells Possessing Stem Cell–Like Self-Renewal and Multipotential Differentiation Capacity

Pietro Randelli,*† MD, Erika Conforti,* MS, Marco Piccoli,* PhD, Vincenza Ragone,* MEng, Pasquale Creo,* BA, Federica Cirillo,* PhD, Pamela Masuzzo,* MD, Cristina Tringali,*‡ MS, Paolo Cabitza,*† MD, Guido Tettamanti,† MD, Nicoletta Gagliano,† PhD, and Luigi Anastasia,*†§ PhD
Investigation performed at the Università degli Studi di Milano, Milan, Italy

Background: Stem cell therapy is expected to offer new alternatives to the traditional therapies of rotator cuff tendon tears. In particular, resident, tissue-specific, adult stem cells seem to have a higher regenerative potential for the tissue where they reside.

Hypothesis: Rotator cuff tendon and long head of the biceps tendon possess a resident stem cell population that, when properly stimulated, may be induced to proliferate, thus being potentially usable for tendon regeneration.

Study Design: Controlled laboratory study.

Methods: Human tendon samples from the supraspinatus and the long head of the biceps were collected during rotator cuff tendon surgeries from 26 patients, washed with phosphate-buffered saline, cut into small pieces, and digested with collagenase type I and dispase. After centrifugation, cell pellets were resuspended in appropriate culture medium and plated. Adherent cells were cultured, phenotypically characterized, and then compared with human bone marrow stromal cells (BMSCs), as an example of adult stem cells, and human dermal fibroblasts, as normal proliferating cells with no stem cell properties.

Results: Two new adult stem cell populations from the supraspinatus and long head of the biceps tendons were isolated, characterized, and cultured in vitro. Cells showed adult stem cell characteristics (ie, they were self-renewing in vitro, clonogenic, and multipotent), as they could be induced to differentiate into different cell types—namely, osteoblasts, adipocytes, and skeletal muscle cells.

Conclusion: This work demonstrated that human rotator cuff tendon stem cells and human long head of the biceps tendon stem cells can be isolated and possess a high regenerative potential, which is comparable with that of BMSCs. Moreover, comparative analysis of the sphingolipid pattern of isolated cells with that of BMSCs and fibroblasts revealed the possibility of using this class of lipids as new possible markers of the cell differentiation status.

Clinical Relevance: Rotator cuff and long head of the biceps tendons contain a stem cell population that can proliferate in vitro and could constitute an easily accessible stem cell source to develop novel therapies for tendon regeneration.

Keywords: stem cells; rotator cuff tendon; sphingolipids; regenerative medicine

Rotator cuff tendons are often prone to lesions and full-thickness tears, as 30% to 50% of the population older than 50 years has partial- or full-thickness rotator cuff tears.[9,27] Although surgical procedures have evolved and improved over the past decades, reruptures are still very common,[26] and the overall failure rates of surgical repair range from 30% to 94%, which is far from being acceptable.[13] Several new "biological" approaches have been developed to overcome this issue, including the use of growth factors,[25] bone morphogenetic proteins,[2] and, more recently, stem cells.[6] Research on stem cells for tissue engineering has bloomed over the past decade, although a therapeutic application in tendon repair has yet to be

§Address correspondence to Luigi Anastasia, IRCCS Policlinico San Donato, piazza Malan 1, 20097 San Donato Milanese (Milano), Italy (e-mail: luigi.anastasia@unimi.it).
*IRCCS Policlinico San Donato, San Donato Milanese, Italy.
†Department of Biomedical Sciences for Health, Università degli Studi di Milano, Milan, Italy.
‡Department of Medical Biotechnology and Translational Medicine, Università degli Studi di Milano, Milan, Italy.
Contributing authors are listed at the end of this article.
Dr Randelli and Dr Conforti contributed equally to this work.
The authors declared that they have no conflicts of interest in the authorship and publication of this contribution.

The American Journal of Sports Medicine, Vol. XX, No. X
DOI: 10.1177/0363546512473572

fully developed.[23] Among adult stem cells, bone marrow stromal cells (BMSCs) are by far the most studied. However, tendon-derived stem cells (TDSCs) have also been found in several animal species, including humans.[3,19] These results have been recently extensively reviewed, underlying the potential of tendon stem cells in tendon lesions and in tissue engineering applications.[19] In fact, it has been demonstrated that tendons have a resident progenitor cell population that possesses several universal characteristics proper of adult stem cells, including clonogenicity, self-renewal, and multipotent differentiation capacity.[3] Although tenocyte-like cells have been recently isolated and cultured in vitro,[24] the isolation of a cell population with stem cell characteristics from the human rotator cuff has yet to be reported. Moreover, although BMSCs have been shown to be able to differentiate into several mesenchymal tissues, including tendons,[12] the possibility of isolating tendon-specific stem cells is desirable, as progenitor cells are more prone to differentiate into those cell types that belong to the tissue in which they reside[32]: they form stem cell reservoirs, the "niches"[10] that can regulate the physiological turnover of differentiated cells, also in organs such as the brain and the heart, which have been recently proven to undergo some regeneration during aging.[5,33] Along this line, a very recent study reported an in-depth comparison of the phenotype and the regenerative potential of rat TDSCs and BMSCs.[31] Interestingly, the authors found that TDSCs possess a higher proliferative rate and multilineage differentiation potential than BMSCs, therefore concluding that TDSCs are a very promising stem cell source for musculoskeletal tissue engineering.

The aim of this study is the isolation and characterization of new adult stem cell populations from the supraspinatus (SS), which is part of the rotator cuff, and from the long head of the biceps (LHB) tendons (Figure 1, A-C). To confirm our hypothesis, it has been necessary that these SS and LHB cells could be cultured and expanded and that they showed adult stem cell characteristics (ie, they are self-renewing in vitro, clonogenic, and multipotent), as they could be induced to differentiate in vitro into different cell types, including osteoblasts, adipocytes, and skeletal muscle cells. These new cell populations should be phenotypically characterized and compared with BMSCs and human dermal fibroblasts (DFs). Moreover, as sphingolipids are emerging key regulatory molecules of stem cell proliferation and differentiation,[15] the sphingolipid pattern of all cells should be determined. Finally, the differentiation potential of these new tendon stem cells should be compared with those of bone marrow stem cells and dermal fibroblasts. In fact, as a variety of stem cell sources have become available, it seems desirable and useful to have comparative data to test their differentiation potential toward different cell types, thus clarifying what works best for the regeneration of a specific tissue.

Therefore, the working hypothesis of this study is that the rotator cuff tendon does possess a resident stem cell population that, when properly stimulated, may be induced to proliferate, thus being potentially usable for tendon regeneration.

MATERIALS AND METHODS

Cell Isolation and Culture

Human tendon samples were collected during arthroscopic rotator cuff repairs as described below. The protocol study was approved by the Hospital Ethical Committee (authorization number 2642; September 19, 2011). Patients were recruited among those electing to undergo an arthroscopic cuff repair. Patients with a rotator cuff tear diagnosed by preoperative magnetic resonance imaging and verified by intraoperative evaluation and who gave written informed consent were included in this study. Both chronic and acute tears were included. The exclusion criterion was the presence of unequivocally diagnosed concomitant disorders of the shoulder, including glenohumeral arthritis, fracture, osteonecrosis, instability, or infection. None of the patients had undergone prior surgery on the affected shoulder. Specimens were obtained from 26 consecutive patients during arthroscopic rotator cuff repairs. There were 10 male and 16 female patients with a mean ± SD age of 60 ± 7 years. The mean duration of symptoms was 26 months (range, 6-96 months). Intra-articular findings of the rotator cuff were classified according to Snyder.[29] There were 18 complete tears (degree: C1-C4), 4 bursal surface lesions (degree: B2-B4), and 4 articular surface lesions (degree: A2-A3). Partial articular and bursal surface lesions were converted to full-thickness tears. Samples were collected from SS and LHB tendons in 20 and 6 patients, respectively (Figure 1, A-C). None of the 2 different tendons were collected from the same patient. Arthroscopic rotator cuff repair was performed by the single-row technique with 1 to 3 suture anchors. Before the repair, a single specimen was taken from the residual tendon. The arthroscope was inserted in the glenohumeral joint, and once the cuff tear was identified, the frayed edge of the tear was debrided until normal tendon fibers were identified. A margin of 4 to 8 mm was removed from the edge of the torn supraspinatus tendon before surgical repair by use of an arthroscopic basket punch. The LHB tissue specimens were harvested from the midportion of the intra-articular part of the LHB by arthroscopic tenotomy of the damaged tendon. Samples from SS and LHB tendons (4-8 mm wide) (Figure 1D) were collected from 26 patients, kept in HypoThermosol (BioLife Solutions, Bothell, Washington) at 4°C, and processed separately within 24 hours, according to the procedure described below.

Samples were washed with phosphate-buffered saline (PBS), cut into small pieces, and digested for 90 minutes with collagenase type I (3 mg/mL; Worthington, Lakewood, New Jersey) and dispase (4 mg/mL; Gibco, Life Technologies, Carlsbad, California) in PBS (Euroclone, Pero, Italy) at 37°C. After centrifugation, cell pellets were resuspended in the following culture medium: α-MEM (Sigma-Aldrich, St Louis, Missouri) supplemented with 2 mM glutamine, 100 IU/mL penicillin, 100 mg/mL streptomycin, and 20% fetal bovine serum (FBS), embryonic stem cell tested and European Union approved (PAA Laboratories, Pasching, Austria). Cells were then filtered with a cell strainer (70 μM; BD Falcon, San Jose, California) and plated in 150-cm^2 dishes. Adherent cells were cultured at 37°C in

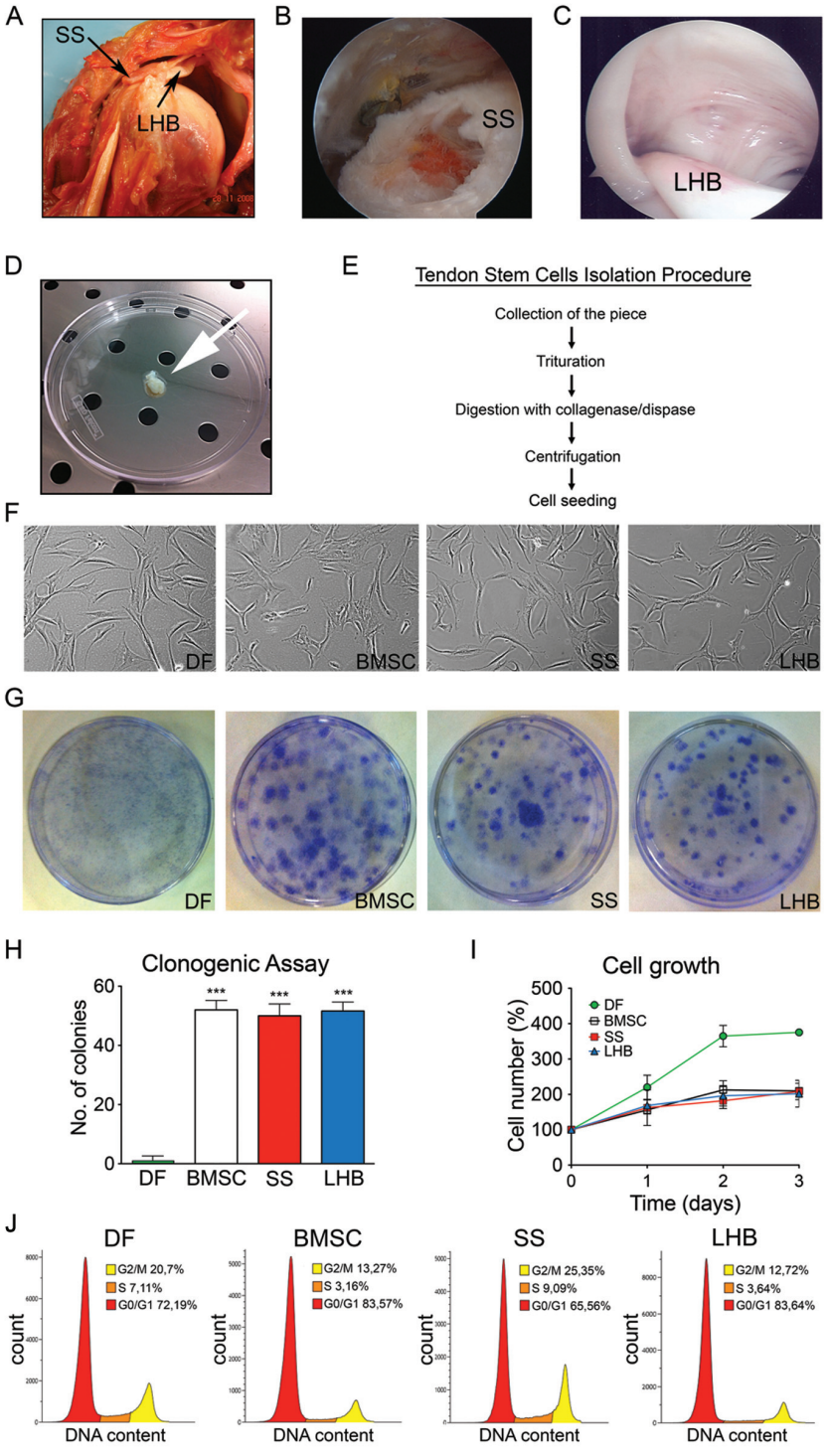

Figure 1. Isolation and characterization of tendon-derived stem cells (TDSCs): comparison with dermal fibroblasts (DFs) and bone marrow stromal cells (BMSCs). (A) Cadaveric picture of shoulder joint with supraspinatus (SS) and long head of the biceps (LHB) tendons indicated by black arrows. (B, C) Representative arthroscopic pictures of the site of fragment collection. (D) Picture of a tendon fragment collected before trituration and processing. (E) Schematic representation of the protocol used to isolate tendon stem cells. (F) Comparative features of TDSCs (SS and LHB) to human DFs and human bone marrow stromal cells (BMSCs): phase-contrast microphotographs (×10 magnification). (G, H) Clonogenic assays and colony-forming efficiency. (I) Cell growth curves and (J) cell cycle analysis of DFs, BMSCs, and SS and LHB cells (G2/M, S, G0/G1). All experiments were performed in triplicates. Error bars show mean ± SD of 3 different experiments (6 in the case of the clonogenic assay); significance according to 2-way ANOVA: ***$P < .001$ compared with DF.

a humidified atmosphere with 5% CO_2. Cells were isolated from all 26 patients. The number of isolated cells from different patients was generally similar and proportional to the tendon fragment size. In all cases, cells could be expanded to at least passage 6 before showing clear signs of senescence. All experiments were carried out at cell passage 3 from seeding. Cells were seeded at 4000 cells/cm^2 density and were passaged when they reached 80% confluence, generally after 48 hours from seeding. Human bone marrow stem cells, obtained from healthy donors, were cultured in low-glucose Dulbecco's modified Eagle's medium (DMEM) supplemented with 4 mM glutamine, 100 IU/mL penicillin, 100 mg/mL streptomycin (all reagents purchased from Sigma-Aldrich), and 10% (v/v) defined FBS (HyClone; Thermo-Fisher Scientific, Waltham, Massachusetts). Human DFs (from ATCC; LGC Standards Srl, Sesto San Giovanni, Italy) and the mouse myogenic cell line C2C12 (ATCC; LGC Standards Srl) were maintained in high-glucose DMEM supplemented with 4 mM glutamine, 100 IU/mL penicillin, 100 mg/mL streptomycin, and 10% (v/v) FBS (Sigma-Aldrich).

Clonogenic Assay

This assay tests the capability of stem cells to form clones starting from single-cell cultures. To this purpose, cells need to be seeded at a very high dilution. Suspensions of 2000 cells (for counts, see below) were plated in 60-mm dishes and cultured for 9 days. Cell colonies were stained with crystal violet (Sigma-Aldrich) for 10 minutes as previously described.[4] Results shown are the average of 6 experiments for each cell type. The DFs and BMSCs were used as controls. We used all 6 different samples of the LHB, as we collected them from 6 patients (3 men and 3 women; average age, 57 years; range, 50-67 years). Therefore, we decided to pick 6 matching samples out of the 20 supraspinatus tendons (3 men and 3 women; average age, 58 years; range, 53-67 years) and tested them separately.

Cell Structure and Growth Curve

For growth curve only, cells were plated at the concentration of 3×10^3 cells/cm^2. Cell structure was examined daily with a phase-contrast microscope (Axiovert 40 CFL; Zeiss, Arese, Italy). Cells were counted at days 1, 2, 3, and 4 with a Countess Cell Counter (Invitrogen; Life Technologies), and cell viability was determined by trypan blue dye exclusion assay.

Flow Cytometry

Isolated cells were characterized by flow cytometry for the expression of key stem cell markers and to test the level of contamination with other cell types. Cell cycle analysis allowed us to test the proliferation status of all studied cells.

Flow cytometry analysis was performed on 2×10^5 cells. Briefly, cells were stained with a 3-step procedure: (1) incubation for 30 minutes at 4°C with 50% FBS (M-Medical, Cornaredo, Italy) in PBS to block the Fc receptor, (2) incubation with conjugated mouse antihuman antibodies at the optimal concentration (1:20 dilution) in PBS for 10 minutes at 4°C, and (3) 2 washes with PBS at 4°C. Samples were analyzed with a Navios cytofluorimeter (Beckman Coulter, Brea, California), and data were processed with Kaluza software (Beckman Coulter). Cell characterization was performed using the following antibodies: αCD9 FITC, αCD73 FITC, αHLA-DR FITC, αCD13 PE, αCD29 PE, αCD45 PE, αCD71 PE, αCD90 PE, αCD105 PE, αPE, α-4 PE, and αCD34 PerCP-eFluor710 (all from eBioscience, San Diego, California); αLineage Cocktail FITC, αCD18 PE, αCD146 PE, and αStro-1 Alexa Fluor 647 (all from BioLegend, San Diego, California); and αCD117 PE (Miltenyi Biotech, Bergisch Gladbach, Germany). Cell cycle analysis was performed on samples containing 10^6 cells. Briefly, cells were fixed in 70% ethanol and kept at 4°C before staining. Cells were then incubated with 10 μg/mL propidium iodide (Propidium Iodide Solution; BioLegend) and diluted in 1 mL PBS, 0.5% Tween 20 (Carlo Erba, Arese, Italy), and 1% bovine serum albumin (Sigma-Aldrich), adding 20 μg/mL RNAse A (Sigma-Aldrich). Staining was performed overnight at 4°C. Samples were analyzed with a Navios cytofluorimeter (Beckman Coulter), and data were processed with Kaluza software.

Real-Time Reverse Transcription Polymerase Chain Reaction

Expression of key markers involved in extracellular matrix remodeling and homeostasis was tested by quantitative polymerase chain reaction (qPCR). Total RNA was isolated by a modification of the acid guanidinium thiocyanate-phenol-chloroform method (Tri-Reagent; Sigma-Aldrich). Total RNA (1 μg) was reverse-transcribed in a 20-μL final volume of reaction mix (BioRad, Hercules, California). The mRNA levels of collagen type I and type III (COL-I, COL-III), matrix metalloproteinase 1 and 2 (MMP-1, MMP-2), transforming growth factor–β1 (TGF-β1), N-cadherin (N-cad), and connexin 43 (Cx43) were assessed. Glyceraldehyde-3-phosphate dehydrogenase (GAPDH) was used as endogenous control to normalize the differences in the amount of total RNA in each sample.

The primer sequences, designed with Beacon Designer 6.0 Software (BioRad), were the following:

GAPDH: FW-CCCTTCATTGACCTCAACTACATG,
REV-TGGGATTTCCATTGATGACAAGC
COL-I: FW-CGACCTGGTGAGAGAGGAGTTG,
REV-AATCCATCCAGACCATTGTGTCC
COL-III: FW-TGTCAAGTCTGGAGTAGCAGTAGG,
REV-GGAACCAGGATGACCAGATGTACC
MMP-1: FW-CGGATACCCCAAGGACATCTACAG,
REV-GCCAATTCCAGGAAAGTCATGTGC
MMP-2: FW-GCAGTGCAATACCTGAACACCTTC,
REV-TCTGGTCAAGATCACCTGTCTGG
TGF-β1: FW-GTGCGGCAGTGGTTGAGC,
REV-GGTAGTGAACCCGTTGATGTCC
N-cad: FW-CTCTCGCCTATGTCTCCTCCTG,
REV-TTTGCTCACTTGCTTGCTTGTTG,
REV-TTGGAGCCTGAGACACGATTCTG
Cx43: FW-CTCTCGCCTATGTCTCCTCCTG,
REV-TTTGCTCACTTGCTTGCTTGTTG

Amplification reactions were conducted in a 96-well plate in a final volume of 20 μL per well containing 10 μL of 1× SYBR Green Supermix (BioRad), 2 μL of template, and 300 pmol of each primer, and each sample was analyzed in triplicate in an iQ5 thermal cycler (BioRad) after 40 cycles. The cycle threshold (Ct) was determined, and gene expression levels relative to that of GAPDH were calculated by the $2^{-\Delta\Delta Ct}$ method, using the Gene Study module of the iQ5 software (BioRad).

Slot Blot

Expression of key markers involved in extracellular matrix remodeling and homeostasis was tested by slot blot. The COL-I and MMP-1 protein levels secreted in cell supernatants by BMSCs and tendon stem cells were assessed by slot blot. For this purpose, cell culture media were concentrated 20-fold with Centricon 10 columns (Amicon Y10; Millipore, Billerica, Massachusetts). Protein content was determined by a standardized colorimetric assay (DC Protein Assay; Bio-Rad); 100 μg of total protein per sample in a final volume of 200 μL Tris-buffered saline (TBS) was spotted onto a nitrocellulose membrane in a Bio-Dot SF apparatus (BioRad). Membranes were blocked for 1 hour with 5% skimmed milk in TBS containing 0.05% Tween 20 (TBST), pH 8, and incubated for 1 hour at room temperature in a monoclonal antibody to COL-I (1:1000 in TBST; Sigma-Aldrich) or to MMP-1 (1 μg/mL in TBST; Millipore). After washing, membranes were incubated in horseradish peroxidase (HRP)–conjugated rabbit antimouse serum (1:40,000 in TBST; Sigma-Aldrich) for 1 hour. Immunoreactive bands revealed by the Amplified Opti-4CN substrate (BioRad) were scanned densitometrically (UVBand, Eppendorf, Hamburg, Germany).

Western Blot

Expression of key proteins involved in extracellular matrix remodeling and homeostasis was tested by Western blot. This technique allowed us to also distinguish the active from the inactive protein forms.

ProMMP-1 and active MMP-1 protein levels were assessed by Western blot. Concentrated culture media (25 μg of total proteins) were diluted in a sodium dodecyl sulfate (SDS) sample buffer, loaded on 10% SDS–polyacrylamide gel, separated under reducing and denaturing conditions at 80 V, and transferred at 90 V to a nitrocellulose membrane in 0.025 M Tris, 192 mM glycine, and 20% methanol, pH 8.3. After electroblotting, the membranes were air dried and blocked for 1 hour. After being washed in TBST, membranes were incubated for 1 hour at room temperature in monoclonal antibody to MMP-1 (1 μg/mL in TBST; Millipore) and, after washing, in HRP-conjugated rabbit antimouse serum (1:40,000 dilution; Sigma-Aldrich). Immunoreactive bands were revealed using the Amplified Opti-4CN substrate.

SDS-Zymography

This technique also allows testing the activity of key proteins of the extracellular matrix. Concentrated culture media were mixed 3:1 with sample buffer (containing 10% SDS). Samples (7 μg of total protein per sample) were run under nonreducing conditions without heat denaturation onto 10% polyacrylamide gel (SDS-PAGE; Bio-Rad) copolymerized with 1 mg/mL of type I gelatin. The gels were run at 4°C. After SDS-PAGE, the gels were washed twice in 2.5% Triton X-100 for 30 minutes each and incubated overnight in a substrate buffer at 37°C (50 mM Tris-HCl, 5 mM $CaCl_2$, 0.02% NaN_3, pH 7.5). The MMP gelatinolytic activity was detected after staining the gels with Coomassie brilliant blue R250, as clear bands on a blue background.

Radiolabeling of Gangliosides and Neutral Glycolipids by [3-^{3}H]sphingosine and Analysis

To study the sphingolipid pattern of isolated cells, we performed metabolic labeling with the radiolabeled precursor [3-^{3}H]sphingosine. Feeding cells with the precursor allowed cells to synthesize radiolabeled sphingolipids that could be easily analyzed and quantified as described below.

Metabolic labeling of cell sphingolipids was achieved with [3-^{3}H]sphingosine (PerkinElmer, Waltham, Massachusetts), as previously described,[1] with a final concentration of 3×10^{-8} M (corresponding to 0.4 μCi/well). Cells (2×10^5 cells per 100-mm dish) were incubated in the presence of [3-^{3}H]sphingosine for a 2-hour pulse followed by a 48-hour chase, a condition warranting a steady-state metabolic condition. At the end of the chase, cells were washed and harvested in ice-cold PBS by scraping. The cell suspensions were frozen and lyophilized. Total lipids from lyophilized cells were extracted twice with 20:10:1 vol/vol (v/v) chloroform/methanol/water. Lipid extracts, dried under a nitrogen stream, were dissolved in 2:1 (v/v) chloroform/methanol and subjected to a 2-phase partitioning with 20% (v/v) water. The aqueous and organic phases obtained were counted for radioactivity, and the contained [^{3}H]sphingolipids were analyzed by high-performance thin-layer chromatography (Kieselgel 60, 20 × 10 cm; Merck GmbH, Darmstadt, Germany), the solvent system 55:20:3 (v/v) chloroform/methanol/water and 60:40:9 (v/v) chloroform/methanol/aqueous $CaCl_2$ (0.2%) for the organic and aqueous phases, respectively. Radioactive lipids were visualized with a Beta-Imager 2000 (Biospace Lab, Paris, France) and identified by comparison with radiolabeled standards. The radioactivity associated with individual lipids was determined with the specific β-Vision software (Biospace Lab).

Osteogenic Differentiation

Cells were plated at the concentration of 3×10^4 cells/cm^2 and treated with the osteogenic medium (10 nM dexamethasone, 10 mM glycerol-2-phosphate, 150 μM L-ascorbic acid-2-phosphate, and 10 nM cholecalciferol, all purchased from Sigma-Aldrich), the medium being changed 3 times a week for 2 weeks. Osteogenic differentiation was assessed by alkaline phosphatase (ALP) staining (Sigma-Aldrich) according to the manufacturer's procedures. The

ALP activity was determined using the Alkaline Phosphatase Detection Kit (Millipore) according to the manufacturer's procedures, and ALP expression was determined by qPCR (ALP: FW-CGCACGGAACTCCTGACC, REV-GCCACCACCACCATCTCG). Total RNA was isolated with the RNeasy Mini kit (Qiagen, Venlo, the Netherlands). The cDNA was synthesized starting from 0.8 μg of RNA, with the iScript cDNA Synthesis Kit (BioRad) according to the manufacturer's instructions. Briefly, 10 ng of total RNA was used as a template for qPCR performed using the iCycler thermal cycler (BioRad). The PCR mixture included 0.2 μM gene-specific primers for human ALP or human YWHAZ (14-3-3 protein zeta/delta), which was used as housekeeper gene, and 50 mM KCl, 20 mM Tris/HCl (pH 8.4), 0.8 mM dNTPs, 0.7 U iTaq DNA Polymerase, 3 mM $MgCl_2$, and SYBR Green (iQ SYBR Green Supermix; BioRad) in a final volume of 20 μL. Amplification and data acquisition were performed using the following cycle conditions: initial denaturation at 95°C for 3 minutes, followed by 40 cycles of 10 seconds at 95°C and 30 seconds at 57°C.

Adipogenic Differentiation

Cells were plated at a concentration of 3×10^4 cells/cm^2 and treated with the Mesenchymal Adipogenisis Kit (Chemicon, Temecula, California), the medium being changed 3 times a week for 3 weeks. Adipogenic differentiation was assessed by evaluating AdipoRed staining (Chemicon) according to the manufacturer's procedures. Adipogenic marker expression was determined by qPCR (lipoprotein lipase [LPL]: FW-AGAGAGAACCAGACTCCAATG, REV-GGCTCCAAG GCTGTATCC; peroxisome proliferator-activated receptor–γ [PPAR-γ]: FW-TTCCTTCACTGATACACTGTCTGC, REV-GGAGTGGGAGTGGTCTTCCATTAC), following the same procedure used for osteogenesis.

Skeletal Muscle Cell Differentiation and Evaluation of Differentiation Markers

Cells were plated at the concentration of 2×10^3 cell/cm^2 in their cell culture medium. After 2 days, cells were washed twice with PBS and twice with DMEM containing 10% FBS. C2C12 myoblasts were then added to stem cells containing plates in a ratio of 5:1. The following day, cocultures were shifted in DMEM supplemented with 2% horse serum. Differentiation was carried out for 7 days. Cells were then fixed with 4% wt/vol (w/v) paraformaldehyde at room temperature for 10 minutes and then permeabilized with 0.1% (w/v) Triton X-100 and 1% (w/v) BSA in PBS for 30 minutes. Cells were incubated for 2 hours at room temperature with the following primary antibodies: antihuman nuclei antibody (Millipore) at 1:400 dilution and anti–myosin heavy chain (MHC) monoclonal antibody (Sigma-Aldrich) at 1:100 dilution. After incubation, cells were washed 3 times in PBS and incubated with the appropriate FITC- or TRIC-conjugated secondary antibodies 1 hour at room temperature. After being washed in PBS, cells were analyzed under a fluorescent microscope. Cell nuclei were counterstained with Hoechst 33342 (1:500) for 15 minutes.

RESULTS

Isolation and Characterization of Tendon Stem Cells

Isolation of SS and LHB stem cells was performed according to the protocol described in the Materials and Methods section and summarized in Figure 1E. Phase-contrast microscopy of plated cells revealed that SS and LHB possessed similar morphologic characteristics, which were also similar to those of BMSCs and DFs (Figure 1F). To test whether cell populations were clonogenic, a typical stem cell feature,[3] 2000-cell suspensions were plated in 60-mm dishes and cultured for 9 days. Cell colonies were visualized using crystal violet staining, revealing that SSs, LHBs, and BMSCs formed adherent colonies, whereas DFs did not form significant colonies, as expected (Figure 1, G and H). Quantitative analysis of clonogenicity, performed by counting the number of colonies per 100-mm dish, revealed similar values for SSs, LHBs, and BMSCs (Figure 1H). Cell growth was analyzed by counting plated cells every 24 hours for 3 days and showed that SSs, LHBs, and BMSCs possess comparable proliferation rates, which were significantly lower than those for DFs, as expected (Figure 1I). Cell cycle analysis by flow cytometry revealed, in all cases, a cell cycle phase distribution (G1-S-G2/M) typical of proliferating cell cultures (Figure 1J).

Tendon Stem Cell Phenotypization

Flow Cytometry Analysis. The LHB and SS cells were phenotypically characterized by flow cytometry (see Supplementary Figure S1, A and B and Figure S2, available online at http://ajs.sagepub.com/supplemental/). The data reported are the average values of all samples studied. In particular, the SS values are the average of all 20 patients, whereas those for LHB are the average of 6 patients. Supplementary Figure S1A shows a representative analysis of each marker, where the graph for each surface marker was chosen so that it better represented the average results obtained from all analyzed samples, which are reported in Supplementary Figure S1B. Results revealed that both cell populations were *lineage* (CD2, CD3, CD11b, CD14, CD15, CD16, CD19, CD56, CD123, and CD235a) negative and also negative for the hematopoietic markers (CD18, CD34, and CD117) and the leukocyte marker CD45, confirming lack of contamination from these cell types. Both LHB and SS cell populations were positive for the BMSC markers CD90, CD44, CD146 but negative for CD18, which was also negative in BMSCs, according to what has been observed for human hamstring-tendon stem cells.[3] Stro-1 (a mesenchymal stem cell marker quite controversial since the antigen recognized by the antibody is still unknown and because of the variability of its expression reported in the literature)[17] was negative in BMSCs and DFs but was expressed by 7% of LHB and 13% of SS stem cells. Vascular cell adhesion molecule 1 (VCAM-1 or

CD106), a cell surface sialoglycoprotein that is downregulated during BMSC differentiation,[18] was expressed by 70% of BMSCs, 13% of LHB stem cells, and 16% of SS stem cells. Analysis of CD106 mRNA levels, performed on all isolated samples by qPCR, confirmed the distribution observed by cytofluorimetry (see Supplementary Figure S1C). The activated leukocyte cell adhesion molecule (ALCAM, CD166), another putative mesenchymal stem cell marker,[20] could be detected by cytofluorimetry in BMSCs and LHB and SS stem cells, as well as in DF cells (Supplementary Figures S1B and S2).

Expression of Genes and Proteins Involved in Extracellular Matrix Remodeling and Homeostasis. Gene expression analysis for COL-I, the main component of tendon extracellular matrix (ECM), revealed increased mRNA levels in SS and LHB tendon stem cells as compared with DFs and BMSCs, and a similar pattern was observed in the gene expression analysis for COL-III (Figure 2A). MMP-1 gene expression was strongly downregulated in BMSCs and SS and LHB stem cells compared with human dermal fibroblasts. By contrast, an opposite pattern was observed for MMP-2, which was significantly upregulated in SS and LHB stem cells and TGF-β1 (Figure 2A).

Genes for cell junction proteins showed a different pattern of expression. N-cad mRNA levels were significantly downregulated in BMSCs and SS and LHB stem cells. Conversely, Cx43 gene expression was higher in BMSCs and SS and LHB stem cells (Figure 2F).

COL-I protein levels in cell supernatants were analyzed by slot blot. Densitometric scanning of immunoreactive bands revealed a very similar COL-I protein expression in all the considered cell types (Figure 2B).

MMP-1 protein levels were analyzed by both slot and Western blot using an antibody that can recognize both pro- (inactive) and active MMP-1 (Figure 2, C and D). The total MMP-1 protein levels were similar in DFs and all stem cell supernatants; in particular, similar levels of proMMP-1 and active MMP-1 were detected. MMP-2 activity analyzed by SDS-zymography resulted in similar DF and stem cell supernatants (Figure 2E).

Sphingolipid Pattern Analysis. The sphingolipid profiles in the organic and aqueous phases in the examined cells, after metabolic radiolabeling with [3-^{3}H]sphingosine, are reported in Supplementary Figure S3 (available online). With regard to the sphingolipid patterns in the organic phase (Supplementary Figure S3, A and B), no significant differences within the different cell populations were observed for sphingomyelin (SM), ceramide (Cer), glucosylceramide (Glc-Cer), and lactosyl-ceramide (LacCer). Instead, and notably, the relative content of α-galactosyllactosylceramide (Gb3) in SS and LHB cells almost doubled that in DFs and BMSCs. On the other hand, the sphingolipid pattern in the aqueous phase (gangliosides) showed remarkable differences within different cell types: GD1a expression in the SS and LHB cells and BMSCs was much lower (5- to 10-fold) than in the DFs, GM1 expression was higher (about 3-fold) in SS than in DF cells, GM2 expression was higher in DF than in the different stem cells, GM3 expression was higher (25%-30%) in BMSCs than in the other cells, and GD3 expression was markedly higher (until over 10-fold) in BMSCs and SS and LHB cells, as compared with DFs, particularly in stem cells from human tendons.

Multipotency Analysis

Multipotency of SS and LHB cells was tested by inducing cell differentiation of these cells toward osteoblasts, adipocytes, and skeletal muscle. DFs and BMSCs were subjected to the same differentiation experiments and were used as controls for comparison with SS and LHB.

Osteogenesis was induced by culturing cells in the appropriate differentiation medium for 3 weeks and detected with alkaline phosphatase activity staining (Figure 3A), as described in the Materials and Methods. Alkaline phosphatase expression was determined by qPCR and revealed a 3- to 4-fold increase for BMSCs and SS cells and a 6-fold increase for LHB cells as compared with DFs (Figure 3B). Alkaline phosphatase activity showed a 2.7-, 2.2-, and 4.8-fold increase for BMSCs and SS and LHB cells, as compared with DFs, respectively (Figure 3B).

Adipogenic differentiation was induced by culturing cells in the appropriate differentiation medium (see Materials and Methods) for 3 weeks. Oil red staining revealed the formation of mature adipocytes in all cultures with the exception of DF (Figure 3C), as expected. Analysis of adipocyte-specific markers PPAR-γ and LPL by qPCR confirmed a significant expression increase of the genes in SS and LHB cells, as compared with DFs, although significantly lower than that observed in BMSCs (Figure 3D). In particular, PPAR-γ showed a 6.9-, 4.7-, and 3.1-fold expression increase while LPL showed a 36.3-, 14.8-, and 12.7-fold increase for BMSCs and SS and LHB cells, as compared with DF, respectively (Figure 3D).

To test whether tendon stem cells possess myogenic competence to differentiate into skeletal muscle, cells were cocultured with C2C12 murine myoblasts, in a 1:4 ratio. Skeletal muscle differentiation was induced as described in the Materials and Methods. Coimmunostaining with human nuclei (green) and MHC (red) antibodies revealed the formation of myotubes incorporating human nuclei (Figure 3E). Control experiments showed that no human nuclei could be detected in myotubes formed by coculturing DFs and C2C12 (Figure 3, E and F). On the other hand, incorporation of human nuclei inside MHC-positive myotubes could be observed with a frequency of roughly 4% for BMSCs and 10% for both SSs and LHBs, calculated by dividing the number of myotubes containing at least 1 human nucleus by the overall number of myotubes for each field (Figure 3, E and F).

DISCUSSION

In this work, 2 new adult stem cell populations from the SS and LHB tendons were isolated, characterized, and cultured in vitro. Cells showed adult stem cell characteristics (ie, they were self-renewing in vitro, clonogenic, and multipotent), as they could be induced to differentiate into different cell types—namely, osteoblasts, adipocytes, and skeletal muscle cells.

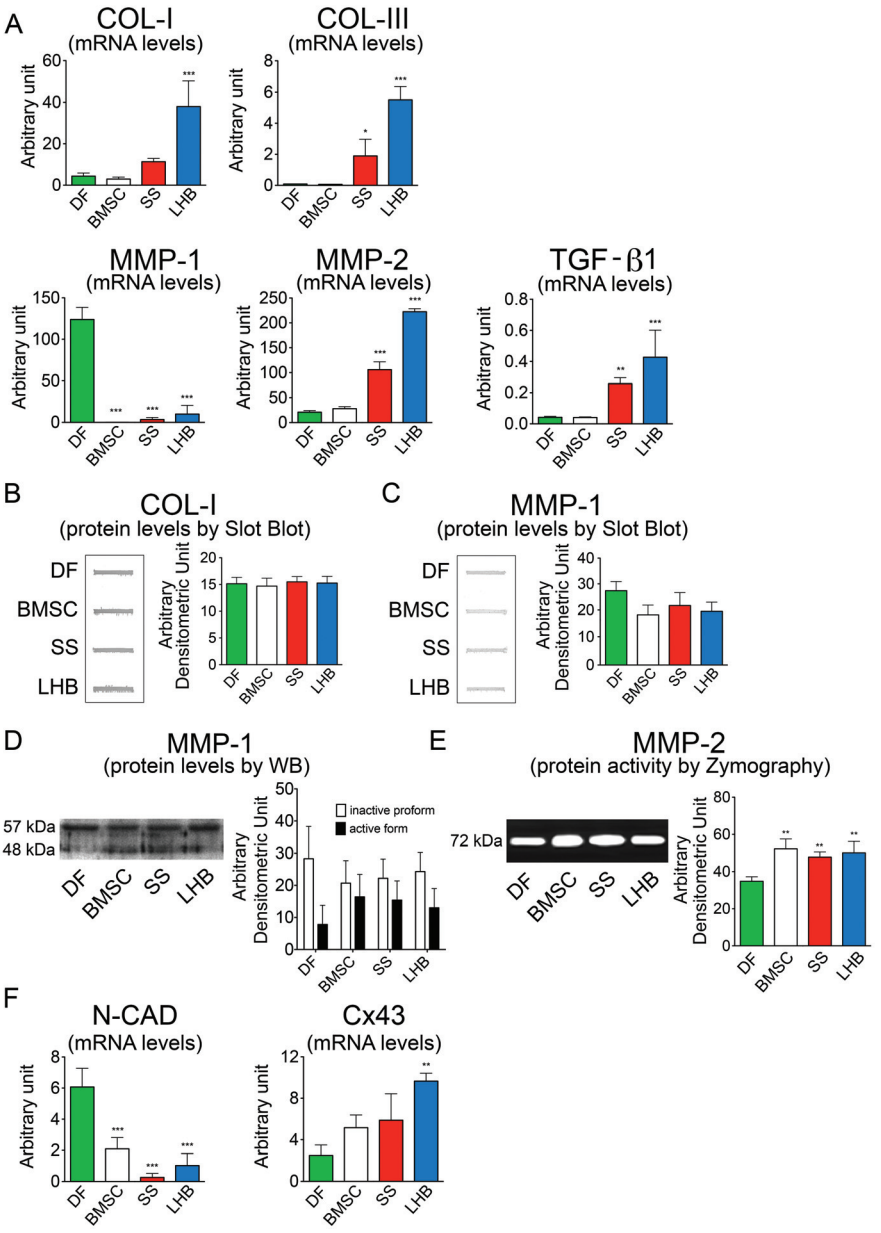

Figure 2. (A) Bar graphs showing collagen type I (COL-I), collagen type III (COL-III), metalloproteinase 1 and 2 (MMP-1 and MMP-2), and transforming growth factor–β1 (TGF-β1) mRNA levels in dermal fibroblasts (DFs), bone marrow stromal cells (BMSCs), and supraspinatus (SS) and long head of the biceps (LHB) cells. Changes in mRNA are normalized to GAPDH gene expression. Values are means ± SD for triplicate samples. (B) Representative slot blot and bar graphs for COL-I protein levels in supernatants from DFs, BMSCs, and SS and LHB cells. Data are means ± SD for triplicate samples. (C) Representative slot blot and bar graphs for MMP-1 protein levels in supernatants of DFs, BMSCs, and SS and LHB cells. Immunoreactive bands were obtained using a monoclonal antibody specific for both pro- and active MMP-1. Data are means ± SD for triplicate samples. (D) Representative Western blot for MMP-1 levels (the immunoreactive bands in the 60/50-kDa region correspond to proMMP-1 and active MMP-1) and bar graphs showing proMMP-1 and MMP-1 protein levels. Data are expressed as densitometric units and are means ± SD. (E) Representative gelatin zymogram of MMP-2 in serum-free, conditioned supernatants from DFs, BMSCs, and SS and LHB cells. The lytic bands in the 72-kDa region correspond to proMMP-2. Bar graphs show MMP-2 activity after densitometric analysis of lytic bands following SDS-zymography. Data are expressed as densitometric units and are means ± SD. Error bars show mean ± SD of 3 different experiments, with significance according to 2-way ANOVA: $*P < .05$, $**P < .01$, and $***P < .001$ compared with DF. (F) Bar graphs showing N-cad and Cx43 mRNA levels in DFs, BMSCs, and SS and LHB cells. Changes in mRNA are normalized to GAPDH gene expression. Values are means ± SD for triplicate samples.

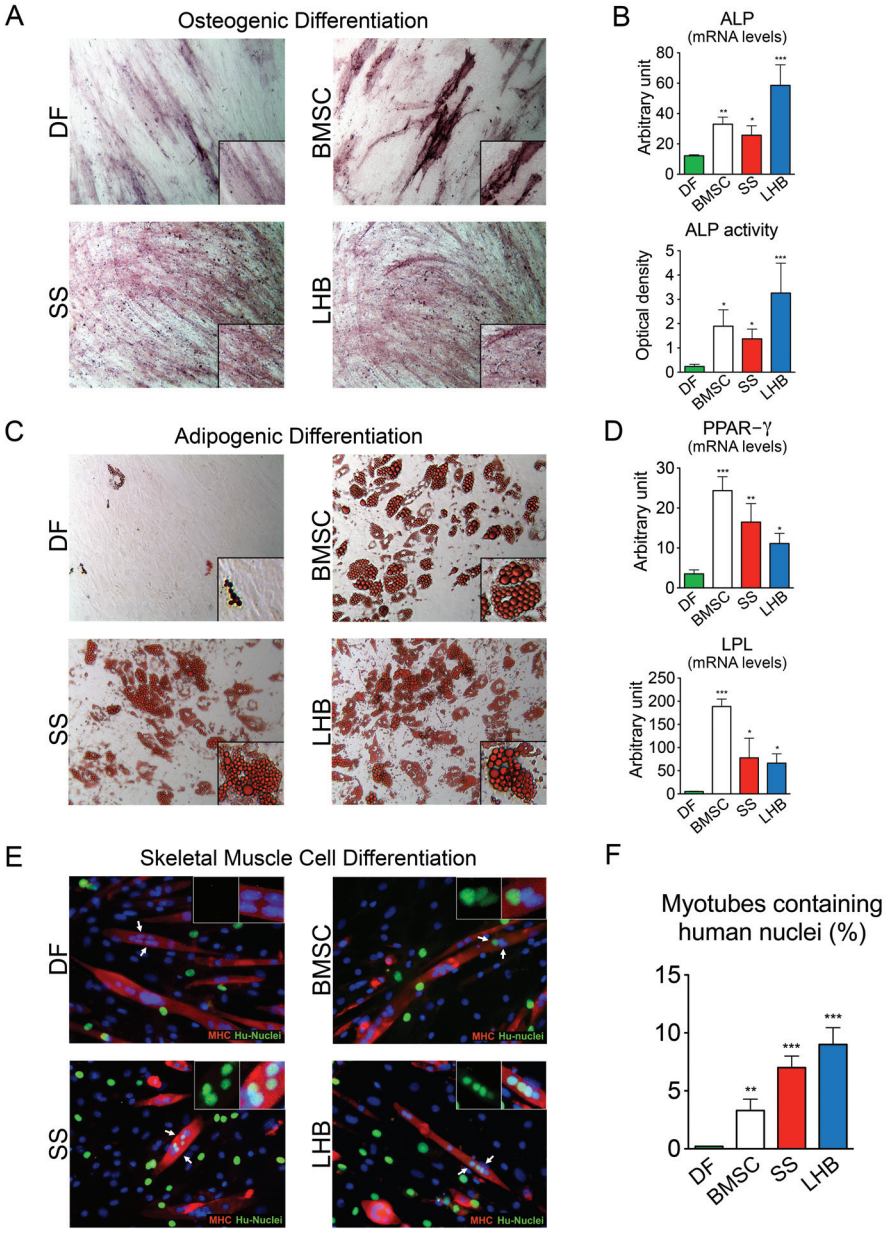

Figure 3. In vitro differentiation of dermal fibroblasts (DFs), bone marrow stromal cells (BMSCs), and supraspinatus (SS) and long head of the biceps (LHB) cells toward the osteogenic (A, B), adipogenic (C, D), and skeletal muscular cell phenotype (E, F). (A) Alkaline phosphatase (ALP) staining revealed the presence of osteoblast-like cells (purple). A typical result is shown. (B) ALP expression by quantitative polymerase chain reaction (qPCR) and ALP enzymatic activity. (C) Lipid vacuoles (red) in the adipocytes were stained with Oil Red O solution. (D) Peroxisome proliferator-activated receptor–γ (PPAR-γ) and lipoprotein lipase (LPL) expression by qPCR. (E) Skeletal muscle differentiation was induced by culturing cells in 2% horse serum medium for 7 days. Coimmunostaining with human nuclei (green) and myosin heavy chain (MHC, red) antibodies and staining of nuclei with Hoechst 33342 (blue) revealed the formation of myotubes incorporating human nuclei (yellow) expressing sarcomeric myosin in the cytoplasm only in BMSCs and SS and LHB cells. (F) Comparison of quantification of the incorporation of human nuclei inside MHC-expressing myotubes was calculated by dividing the number of myotubes containing at least 1 human nucleus of myotubes for each field. All quantitative data represent means ± SD of 3 different experiments (significance according to 2-way ANOVA: $*P < .05$, $**P < .01$, and $***P < .001$ compared with DFs). Hu, human.

Rotator cuff tendon tears still suffer from the lack of reliable alternative approaches to surgery and could greatly benefit from the development of a stem cell–based therapy. In general, tendon progenitor cells may represent a new, endogenous, patient-specific stem cell source for tissue regeneration. Like most other tissue-specific stem cells, they are normally present in small numbers in adult tissues and are in a quiescent state until properly stimulated. With the present investigation, we report that stem cells from the SS can be easily isolated, cultured, and expanded in vitro. We name this family of stem cells *human rotator cuff stem cells* (HRCSCs). Moreover, we also isolated stem cells from the LHB, with a proliferation and differentiation potential almost superimposable to that of SS. We name this family of stem cells *human long head of the biceps stem cells* (HLHBSCs). Thus, the possibility of collecting LHB tendon fragments during rotator cuff surgeries could be envisioned, particularly in those patients in whom the LHB tendon is also damaged and is normally discarded during surgery. This approach represents an alternative to the use of BMSCs, as tendon stem cells could be collected in the same site of injury and at the same time of tendon surgery, without requiring additional invasive procedures in other sites. Moreover, these cells would be the same cells that are endogenously activated after injury and might be induced to differentiate into tenocytes by the inflammatory response. Therefore, they are expected to have a better regenerative potential than other stem cell sources coming from other tissues. This issue was also faced in our investigation with a comparative analysis of the differences at the molecular level among SS and LHB stem cells, BMSCs, and DFs to reveal common and different features. In particular, *tissue-specific* and *stem cell* markers were analyzed by cytofluorimetry, revealing that SS and LHB cells are very similar to each other, but they differ from BMSCs in the expression level of key stem cell markers such as CD106 and Stro-1. How these differences would affect the regenerative potential of these cells is a matter for further investigation. In the search of further characterization of the 2 newly isolated tendon stem cell populations, the sphingolipid patterns of all cell types used were determined and compared. The levels of sphingomyelin, ceramide, glucosylceramide, and lactosylceramide were very similar in all the different cells, whereas Gb3 was markedly more abundant in SS and LHB tendon stem cells as compared with BMSCs and DFs, which exhibited very similar contents. This finding, potentially interesting, requires further investigation. The ganglioside pattern also showed remarkable differences: GD1a level was markedly lower in all stem cells, including SS and LHB stem cells, as compared with proliferating human fibroblasts, whereas GD3 was much more abundant in all stem cells, particularly in LHB cells, as compared with DFs. These novel findings, which deserve more detailed investigations, further corroborate the notion that glycosphingolipids, particularly gangliosides, present on the plasma membrane and often enriched in the lipid rafts, are involved in the regulation of key receptors implicated in cell differentiation and proliferation.[15,16,35] These results are also in accordance with other studies reporting the involvement of GD1a in stem cell differentiation, where its increase was necessary for the progression of the process.[36] Overall, increasing evidence seems to support the hypothesis that GD1a levels could be a direct expression of the differentiation stage of a stem cell.

The newly isolated tendon stem cells were also analyzed for their phenotype in relation to their activity in ECM remodeling, since ECM plays a key role in maintaining tendon structure and biomechanical properties. COL-I is the main component of the dense connective tissue of tendons, accounting for 60% to 80% of the dry mass.[11] COL-I and COL-III mRNA levels were both upregulated in SS and LHB stem cells, compared with DFs and BMSCs, according to TGF-β1 gene expression.[8] It is interesting to note significant differences in COL-I and COL-III expression between SS and LHB. As many factors could influence COL-I and COL-III expression in vitro, including the choice of the culturing medium, understanding the reasons for the observed differential expression will require further investigation. Also, a therapeutic potential was recently suggested for PRGFs,[7] containing many growth factors acting on ECM turnover to enhance the repair of supraspinatus tendon enthesis. Although TGF-β1 is the main growth factor inducing fibroblast proliferation and ECM components synthesis, we cannot speculate on the possible local delivery of TGF-β1 to induce tendon healing for 2 main reasons. First, the intermediate portion of tendons has a structure completely different from the structure of enthesis. Second, the uncontrolled and persistent activity of TGF-β1 could be responsible for the unbalanced deposition of collagen and ECM components in tendons. COL-I and COL-III induction was described as a regenerative and healing response in injured tendons.[21] Our data showing COL-I and COL-III mRNA level upregulation in SS and LHB tendon stem cells seem to suggest for these cells a greater ability for tendon healing compared with BMSCs. However, this hypothesis was not confirmed by the analysis of COL-I protein levels, the main collagen type in tendons, since the expression of COL-I at the protein level was similar in all the considered cell types. The inconsistency of COL-I mRNA and protein levels in BMSCs and LHB and SS stem cells and the finding of unmodified COL-I protein levels in all cell supernatants suggests a different posttranscription and/or posttransduction regulation of the COL-I gene in tendon stem cells. Collagen content is dependent on the finely regulated dynamic balance between its synthesis and degradation by MMPs. MMP-1 is necessary to begin the collagen degradation pathway since it can cleave the native triple helical region of interstitial collagens into characteristic 3/4- and 1/4-collagen degradation fragments, also known as gelatins,[28] that can be further degraded by less specific proteinases such as MMP-2, leading to complete digestion of the fibrillary collagen.[34] MMP-1 and MMP-2 protein levels and activity were similar in all the considered cell supernatants, as observed for COL-I protein expression. These findings suggest that SS and LHB cells are characterized by increased COL-I mRNA levels compared with DF and BMSC cells but have similar COL-I, MMP-1, and MMP-2

protein expression. We can therefore hypothesize a different regulation for the COL-I gene, possibly occurring at a posttranscription or maturation level. Moreover, as tenocytes are arranged in longitudinal rows between the fiber bundles in mature tendons, they are intimately connected cell to cell with neighboring cells, both with the same cell row and with parallel rows, containing adherens and gap junctions formed by Cx32 and Cx43.[22] Therefore, N-cad is the transmembrane protein of adherens junctions in mesenchymal cells, supported by the actin cytoskeleton, that contributes to cell-cell interaction and to mechanotransduction mechanisms in response to mechanical load.[14] Analysis of N-cad mRNA levels revealed a higher expression in DFs, which is consistent with an increased cell-cell adhesion or cell-matrix adhesion, as compared with both BMSCs and tendon stem cells. This suggests that adult fibroblasts are involved in maintaining the integrity of the longitudinal tendon rows and monitoring tensile load more than stem cells and that BMSCs and tendon stem cells display a similar phenotype in relation to N-cad expression.

Cx43 allows cell communication both longitudinally and laterally, contributing to the maintenance of tendon ECM homeostasis in response to tendon mechanical loading, allowing coordination of synthetic activity and facilitating strain-induced collagen synthesis. Our results show an increased Cx43 gene expression in BMSCs and SS and LHB tendon stem cells compared with DF. According to a previous study, which showed Cx43 mRNA upregulation in immature tendons,[30] we can hypothesize that tendon stem cells are immature cells having a high Cx43 expression to provide a sustained gap-junction communication that is necessary for the differentiation process.

Overall, our results confirmed that both SSs and LHBs could be efficiently induced to differentiate into osteoblasts, adipocytes, and even skeletal muscle cells, where bone marrow stem cells gave poor results. Further studies to test the differentiation potential of SS and LHB stem cells in vivo are now necessary to understand their full potential in regenerative medicine.

CONTRIBUTING AUTHORS

Sonia Bergante, MS, Andrea Ghiroldi, PhD (IRCCS Policlinico San Donato, San Donato Milanese, Italy).

REFERENCES

1. Anastasia L, Papini N, Colazzo F, et al. NEU3 sialidase strictly modulates GM3 levels in skeletal myoblasts C2C12 thus favoring their differentiation and protecting them from apoptosis. *J Biol Chem*. 2008;283(52):36265-36271.
2. Bedi A, Maak T, Walsh C, et al. Cytokines in rotator cuff degeneration and repair. *J Shoulder Elbow Surg*. 2012;21(2):218-227.
3. Bi Y, Ehirchiou D, Kilts TM, et al. Identification of tendon stem/progenitor cells and the role of the extracellular matrix in their niche. *Nat Med*. 2007;13(10):1219-1227.
4. Bi Y, Stuelten CH, Kilts T, et al. Extracellular matrix proteoglycans control the fate of bone marrow stromal cells. *J Biol Chem*. 2005;280(34):30481-30489.
5. Chen J. Hematopoietic stem cell development, aging and functional failure. *Int J Hematol*. 2011;94(1):3-10.
6. Grange S. Current issues and regulations in tendon regeneration and musculoskeletal repair with mesenchymal stem cells. *Curr Stem Cell Res Ther*. 2012;7(2):110-114.
7. Hoppe S, Alini M, Benneker LM, Milz S, Boileau P, Zumstein MA. Tenocytes of chronic rotator cuff tendon tears can be stimulated by platelet-released growth factors [published online April 20, 2012]. *J Shoulder Elbow Surg*. doi:10.1016/j.jse.2012.01.016.
8. Ignotz RA, Massague J. Transforming growth factor–beta stimulates the expression of fibronectin and collagen and their incorporation into the extracellular matrix. *J Biol Chem*. 1986;261(9):4337-4345.
9. Isaac C, Gharaibeh B, Witt M, Wright VJ, Huard J. Biologic approaches to enhance rotator cuff healing after injury. *J Shoulder Elbow Surg*. 2012;21(2):181-190.
10. Isern J, Mendez-Ferrer S. Stem cell interactions in a bone marrow niche. *Curr Osteoporos Rep*. 2011;9(4):210-218.
11. Kannus P. Structure of the tendon connective tissue. *Scand J Med Sci Sports*. 2000;10(6):312-320.
12. Kida Y, Morihara T, Matsuda KI, et al. Bone marrow–derived cells from the footprint infiltrate into the repaired rotator cuff [published online April 28, 2012]. *J Shoulder Elbow Surg*. doi:10.1016/j.jse.2012.02.007.
13. Kim HM, Galatz LM, Das R, Havlioglu N, Rothermich SY, Thomopoulos S. The role of transforming growth factor beta isoforms in tendon-to-bone healing. *Connect Tissue Res*. 2011;52(2):87-98.
14. Kjaer M. Role of extracellular matrix in adaptation of tendon and skeletal muscle to mechanical loading. *Physiol Rev*. 2004;84(2):649-698.
15. Kwak DH, Seo BB, Chang KT, Choo YK. Roles of gangliosides in mouse embryogenesis and embryonic stem cell differentiation. *Exp Mol Med*. 2011;43(7):379-388.
16. Liang YJ, Kuo HH, Lin CH, et al. Switching of the core structures of glycosphingolipids from globo- and lacto- to ganglio-series upon human embryonic stem cell differentiation. *Proc Natl Acad Sci U S A*. 2010;107(52):22564-22569.
17. Lin G, Liu G, Banie L, et al. Tissue distribution of mesenchymal stem cell marker Stro-1. *Stem Cells Dev*. 2011;20(10):1747-1752.
18. Liu F, Akiyama Y, Tai S, et al. Changes in the expression of CD106, osteogenic genes, and transcription factors involved in the osteogenic differentiation of human bone marrow mesenchymal stem cells. *J Bone Miner Metab*. 2008;26(4):312-320.
19. Lui PP, Chan KM. Tendon-derived stem cells (TDSCs): from basic science to potential roles in tendon pathology and tissue engineering applications. *Stem Cell Rev*. 2011;7(4):883-897.
20. Majumdar MK, Thiede MA, Mosca JD, Moorman M, Gerson SL. Phenotypic and functional comparison of cultures of marrow-derived mesenchymal stem cells (MSCs) and stromal cells. *J Cell Physiol*. 1998;176(1):57-66.
21. Matthews TJ, Hand GC, Rees JL, Athanasou NA, Carr AJ. Pathology of the torn rotator cuff tendon: reduction in potential for repair as tear size increases. *J Bone Joint Surg Br*. 2006;88(4):489-495.
22. McNeilly CM, Banes AJ, Benjamin M, Ralphs JR. Tendon cells in vivo form a three dimensional network of cell processes linked by gap junctions. *J Anat*. 1996;189(pt 3):593-600.
23. Nixon AJ, Watts AE, Schnabel LV. Cell- and gene-based approaches to tendon regeneration. *J Shoulder Elbow Surg*. 2012;21(2):278-294.
24. Pauly S, Klatte F, Strobel C, et al. Characterization of tendon cell cultures of the human rotator cuff. *Eur Cell Mater*. 2010;20:84-97.
25. Randelli P, Arrigoni P, Ragone V, Aliprandi A, Cabitza P. Platelet rich plasma in arthroscopic rotator cuff repair: a prospective RCT study, 2-year follow-up. *J Shoulder Elbow Surg*. 2011;20(4):518-528.
26. Randelli P, Spennacchio P, Ragone V, Arrigoni P, Casella A, Cabitza P. Complications associated with arthroscopic rotator cuff repair: a literature review. *Musculoskelet Surg*. 2012;96(1):9-16.
27. Riley G. The pathogenesis of tendinopathy: a molecular perspective. *Rheumatology (Oxford)*. 2004;43(2):131-142.
28. Sakai T, Gross J. Some properties of the products of reaction of tadpole collagenase with collagen. *Biochemistry*. 1967;6(2):518-528.

29. Snyder SJ. *Shoulder Arthroscopy*. 2nd ed. Philadelphia, PA: Lippincott Williams & Wilkins; 2002.
30. Stanley RL, Fleck RA, Becker DL, Goodship AE, Ralphs JR, Patterson-Kane JC. Gap junction protein expression and cellularity: comparison of immature and adult equine digital tendons. *J Anat*. 2007;211(3):325-334.
31. Tan Q, Lui PP, Rui YF, Wong YM. Comparison of potentials of stem cells isolated from tendon and bone marrow for musculoskeletal tissue engineering. *Tissue Eng Part A*. 2012;18(7-8):840-851.
32. Wagers AJ. The stem cell niche in regenerative medicine. *Cell Stem Cell*. 2012;10(4):362-369.
33. Wang YZ, Plane JM, Jiang P, Zhou CJ, Deng W. Concise review: quiescent and active states of endogenous adult neural stem cells: identification and characterization. *Stem Cells*. 2011;29(6):907-912.
34. Woessner JF Jr. Matrix metalloproteinases and their inhibitors in connective tissue remodeling. *FASEB J*. 1991;5(8):2145-2154.
35. Yanagisawa M. Stem cell glycolipids. *Neurochem Res*. 2011; 36(9):1623-1635.
36. Yang HJ, Jung KY, Kwak DH, et al. Inhibition of ganglioside GD1a synthesis suppresses the differentiation of human mesenchymal stem cells into osteoblasts. *Dev Growth Differ*. 2011;53(3):323-332.